COLOR-IMAGE WATERMARKING USING MULTIVARIATE POWER-EXPONENTIAL DISTRIBUTION

Roland Kwitt and Peter Meerwald and Andreas Uhl

Department of Computer Sciences
University of Salzburg, A-5020 Salzburg, Austria

ABSTRACT

In this paper we present a novel watermark detector for additive spread-spectrum watermarking in the wavelet transform domain of color images. We propose to model the highly correlated DWT subbands of the RGB color channels by multivariate power-exponential distributions. This statistical model is then exploited to derive a likelihood ratio test for watermark detection. Our results indicate that joint statistical modeling of color DWT detail subbands leads to increased detection performance compared to previous approaches, namely watermarking of the luminance channel only, decorrelating the color bands, or relying on a joint Gaussian host signal model.

***Index Terms*—** Watermark Detection, Power-Exponential Distribution, Color Images, Wavelet Transform

1. INTRODUCTION

Watermarking has been proposed as a technology to ensure copyright protection by embedding an imperceptible, yet detectable signal in digital multimedia content such as images or video. Most of the watermarking research focuses on grayscale images. The extension to color image watermarking is usually accomplished by marking only the luminance channel or by processing each color channel separately [1]. Alternatively, the watermark can be embedded only in certain bands such as the blue channel since the human eye is less sensitive to this frequency range [2]. Nevertheless, for best detection performance all color channels should contribute to the watermark signal.

For blind watermarking, i.e. when detection is performed without reference to the unwatermarked host signal, the host interferes with the watermark signal. Detection performance can be significantly improved by accurately modeling the host signal noise [3]. However, expressing the joint statistical distribution of transform coefficients across correlated color channels for watermark detection is tedious and has so far been proposed for the Gaussian host signal case only [4].

The contribution of our work is the derivation of a novel watermark detection scheme for color image watermarking. We propose to use a multivariate statistical model to accurately capture wavelet detail subband statistics and dependencies across RGB color channels. We observe that watermark detection performance is improved compared to watermarking the luminance channel only, decorrelating the color bands, or relying on a joint Gaussian host signal model.

The remainder of this paper is structured as follows: Section 2 gives a brief overview of related work on the topic of color image watermarking. In Section 3 we introduce the statistical model, derive the novel watermark detector and discuss parameter estimation

as well as threshold computation. Section 4 presents experimental results and a comparative study, followed by a summary of the main points and an outlook on future research in Section 5.

2. WATERMARK DETECTION IN COLOR IMAGES

Most of the watermarking research focuses on grayscale image watermarking. For color images, it is common practice to mark the luminance band, disregarding the chromatic bands. However, it is well known that the human visual system is least sensitive to the yellow-blue channel in the opponent representation of color, thus the watermark signal should be allocated to that band [2, 5]. In this paper we focus not on perceptual shaping of the watermark signal but on detecting the watermark in highly correlated color channels where the watermark is embedded with constant strength. A direct application might be a CMOS image sensor with watermarking capabilities [6] adding a spread-spectrum watermark to RGB data.

Barni et al. [4] investigate color watermarking in the full-frame DCT domain and compare against luminance-channel only watermarking. The same watermark sequence is added to the mid-frequency transform coefficients of all three RGB bands. On the detector side, they employ a linear correlator (LC) and take into account the correlation between color channels for the computation of the detection threshold. Even for the simple LC detector, the derivation of the detection statistic parameters under the null-hypothesis (no watermark) is quite involved. Therefore, the same authors consider to decorrelate the RGB color bands using the Karhunen-Loeve Transform (KLT) so that a joint statistical model of the multi-channel image coefficients becomes feasible [1]. They employ a Weibull model for the absolute values of DFT transform coefficients and derive a Likelihood-Ratio Test (LRT) assuming the transform coefficients are statistically independent. Some caution is in place here: first, decorrelating the color channels does not guarantee that the transform domain coefficients across bands are mutually decorrelated as well [7], and second, decorrelation does not imply statistical independence.
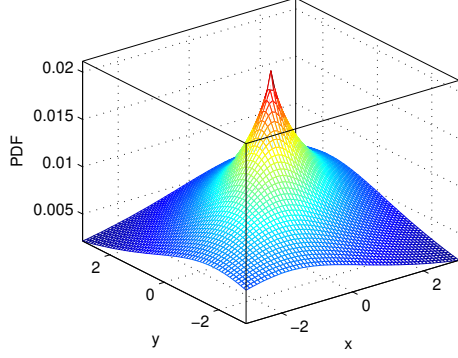
It is well known that DWT and DCT coefficients of a single color channel can be accurately modeled by a Generalized Gaussian Distribution (GGD), leading to improved detection performance [3]. In the next section, we derive a detector based on the multivariate power-exponential (MPE) distribution jointly modeling the DWT subband coefficients of color images. For a comparative study on detection performance, we implement the watermarking approaches described above [4, 1, 3] in the DWT domain.

3. STATISTICAL WATERMARK DETECTION

In this section we introduce a Likelihood-Ratio Test for watermark detection in host signal noise which follows a multivariate power-

Fig. 1. PDF of $\mathrm{MPE}_2\left(\mathbf{0}, \boldsymbol{\Sigma}, 0.4\right)$

Fig. 2. Scatter-plot of the HL subband coefficients of the R,G and B channel of the *Island* image at decomposition level two.

exponential (MPE) distribution and discuss threshold determination as well as parameter estimation issues. This noise model for wavelet detail subband coefficients has already been successfully applied in the context of statistical color image retrieval [8] for example. In the remainder of the paper, we follow the convention that small boldface letters, such as $\mathbf{x}$, denote vectors and big boldface letters, such as $\boldsymbol{\Sigma}$, denote matrices. First, the probability density function (PDF) of the multivariate power-exponential distribution with dimensionality n (MPE_n) is given by

$$p(\mathbf{x}; \boldsymbol{\mu}, \boldsymbol{\Sigma}, \beta) = \frac{n\Gamma\left(\frac{n}{2}\right)}{\pi^{n/2}\Gamma\left(1+\frac{n}{2\beta}\right)2^{1+\frac{n}{2\beta}}} \cdot$$
$$|\boldsymbol{\Sigma}|^{-1/2}\exp\left\{-\frac{1}{2}\left[(\mathbf{x}-\boldsymbol{\mu})^T\boldsymbol{\Sigma}^{-1}(\mathbf{x}-\boldsymbol{\mu})\right]^\beta\right\} \quad (1)$$

where $\boldsymbol{\Sigma}$ is a positive-definite symmetric $n \times n$ matrix, $\beta \in (0, \infty)$ denotes the shape parameter and $\boldsymbol{\mu} \in \mathbb{R}^n$ denotes the location vector. The PDF of a $\mathrm{MPE}_2\left(\mathbf{0}, \boldsymbol{\Sigma}, 0.4\right)$ with $\boldsymbol{\Sigma} = \left(\begin{smallmatrix} 1 & 0.6 \\ 0.6 & 1 \end{smallmatrix}\right)$ is shown in Figure 1. We can reduce the number of free parameters: since we aim at modeling wavelet coefficient distributions, it is reasonable to assume zero mean. Second, we try to capture the joint distribution of wavelet coefficients from subbands of the same orientation and scale but from different color channels. We assume RGB images, thus we have three color bands and $n = 3$. The main reason for choosing a multivariate statistical model is the high correlation which can be observed between the same wavelet detail subbands of different color image channels (see Fig. 2). On all our test images (see Fig. 4) we observe a linear correlation of ≥ 0.8. We further note that the statistical model of Eq. (1) is a special case of the Kotz-type family of distributions (see [9] for example). In what follows, we write $X \sim \mathrm{MPE}_n(\boldsymbol{\Sigma}, \beta)$ when X follows a $\mathrm{MPE}_n(\mathbf{0}, \boldsymbol{\Sigma}, \beta)$ distribution.
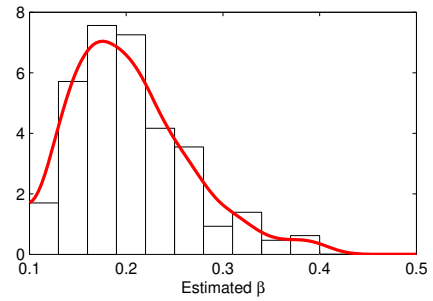
3.1. Parameter Estimation

In this work parameter estimation of the MPE_n noise model is accomplished using the method of moments by matching the variance and Mardia's multivariate Kurtosis coefficient [10, 11] to their empirical estimates. Let $X \sim \mathrm{MPE}_n(\boldsymbol{\Sigma}, \beta)$, then the variance of X, denoted by $\mathbb{V}(X)$, is given by

$$\mathbb{V}(X) = \frac{2^{\frac{1}{\beta}}\Gamma\left(\frac{n+2}{2\beta}\right)}{n\Gamma\left(\frac{n}{2\beta}\right)}\boldsymbol{\Sigma}. \quad (2)$$
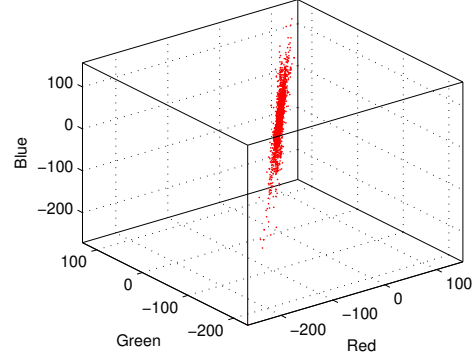
Fig. 3. Histogram and kernel density fit for the shape parameter $\hat{\beta}$ over all 24 Kodak test images.

Mardia's multivariate Kurtosis coefficient is defined as

$$\gamma_2(X) = \mathbb{E}\left[\left((X-\boldsymbol{\mu})^T\boldsymbol{\Sigma}^{-1}(X-\boldsymbol{\mu})\right)^2\right] - n(n+2) \quad (3)$$

which leads to

$$\gamma_2(X) = \frac{n^2\Gamma\left(\frac{n}{2\beta}\right)\Gamma\left(\frac{n+4}{2\beta}\right)}{\Gamma^2\left(\frac{n+2}{2\beta}\right)} - n(n+2) \quad (4)$$

in case of a $\mathrm{MPE}_n(\boldsymbol{\Sigma}, \beta)$ distribution. Given that $\mathbf{S}$ denotes the classic sample variance (setting $\boldsymbol{\mu} = \mathbf{0}$) we can estimate $\gamma_2(X)$ by

$$\hat{\gamma}_2(\mathbf{x}_1, \ldots, \mathbf{x}_m) = \frac{1}{m}\sum_{i=1}^{m}\left(\mathbf{x}_i^T\mathbf{S}^{-1}\mathbf{x}_i\right)^2 - n(n+2). \quad (5)$$

from our data $\mathbf{x}_1, \ldots, \mathbf{x}_m$ where m denotes the number of wavelet coefficients in each target subband. In the first step we estimate β and then use $\hat{\beta}$ to obtain an estimate for $\boldsymbol{\Sigma}$. Figure 3 shows a histogram of the estimated shape parameters over a range of test images. We note that $\beta = 1$ corresponds to a multivariate Gaussian distribution.

3.2. Watermark Embedding and Detection Problem

After decomposing all three color channels separately, we arrange the wavelet coefficients of the three second-level HL subbands columnwise in a $m \times 3$ signal matrix $\mathbf{X}$. To generate the watermark matrix, we first create a bipolar, one-dimensional

pseudo-random watermark sequence $\mathbf{w} = [w_1, \ldots, w_m]^T$ with elements $w_i \in \{+1, -1\}$ (depending on a secret key K). This sequence is used to construct a $m \times 3$ dimensional watermark matrix $\mathbf{W} = [\mathbf{w}^T \ \mathbf{w}^T \ \mathbf{w}^T]$ by columnwise duplicating the watermark vector (column vector). According to the rule of additive spread-spectrum watermarking, $\mathbf{W}$ is then added to the signal matrix by $\mathbf{Y} = \mathbf{X} + \alpha \mathbf{W}$, where $\alpha \in \mathbb{R}_+$ denotes the embedding strength. We could choose a separate embedding strength for each signal dimension, but for the sake of readability we focus on the most simple case here. Based on this watermarking setting, we can now formulate the two hypothesis for our signal detection problem:

$$\mathcal{H}_0 : \mathbf{Y} = \mathbf{X} \quad \text{(not watermarked)}$$
$$\mathcal{H}_1 : \mathbf{Y} = \mathbf{X} + \alpha \mathbf{W} \quad \text{(watermarked)}$$
(6)

Here, $\mathcal{H}_0$ is termed the null-hypothesis (not watermarked) and $\mathcal{H}_1$ denotes the alternative hypothesis (watermarked). By assuming independence of the observations $\mathbf{x}_1, \ldots, \mathbf{x}_m$ we formulate the statistic of the likelihood-ratio test as follows:

$$l(\mathbf{Y}) = \frac{\prod_{i=1}^m p(\mathbf{y}_i - \alpha \mathbf{w}_i; \mathbf{\Sigma}, \beta)}{\prod_{i=1}^m p(\mathbf{y}_i; \mathbf{\Sigma}, \beta)}.$$
(7)

After taking the logarithm and inserting the PDF of Eq. (1) we obtain the detection statistic

$$L(\mathbf{Y}) = -\frac{1}{2} \sum_{i=1}^m \left((\mathbf{y}_i - \alpha \mathbf{w}_i)^T \mathbf{\Sigma}^{-1} (\mathbf{y}_i - \alpha \mathbf{w}_i) \right)^\beta +$$
$$\frac{1}{2} \sum_{i=1}^m \left(\mathbf{y}_i^T \mathbf{\Sigma}^{-1} \mathbf{y}_i \right)^\beta.$$
(8)

By considering all terms of the summation as independent, we can apply the central limit theorem and conclude that $L(\mathbf{Y})$ follows a Normal distribution under both hypothesis $\mathcal{H}_0$ and $\mathcal{H}_1$ with parameters (μ_0, σ_0^2) and (μ_1, σ_1^2), resp. If we consider $\mathbf{y}_i$ as fixed, the only variable term left is $\mathbf{w}_i$ and the expected value μ_0 under $\mathcal{H}_0$ (note that $\mathbf{y}_i = \mathbf{x}_i$) can be calculated as

$$\mu_0 = -\frac{1}{4} \sum_{i=1}^m \left((\mathbf{x}_i - \alpha)^T \mathbf{\Sigma}^{-1} (\mathbf{x}_i - \alpha) \right)^\beta +$$
$$\left((\mathbf{x}_i + \alpha)^T \mathbf{\Sigma}^{-1} (\mathbf{x}_i + \alpha) \right)^\beta + \frac{1}{2} \sum_{i=1}^m \left(\mathbf{x}_i^T \mathbf{\Sigma}^{-1} \mathbf{x}_i \right)^\beta \quad (9)$$

and the variance σ_0^2 of the detection statistic $L(\mathbf{Y})$ is given by

$$\sigma_0^2 = \frac{1}{16} \sum_{i=1}^m \left(\left[(\mathbf{x}_i + \alpha)^T \mathbf{\Sigma}^{-1} (\mathbf{x}_i + \alpha) \right]^\beta - \right.$$
$$\left. \left[(\mathbf{x}_i - \alpha)^T \mathbf{\Sigma}^{-1} (\mathbf{x}_i - \alpha) \right]^\beta \right)^2. \quad (10)$$

The derivation can be found in appendix A. Having obtained both parameters of the Gaussian distribution under $\mathcal{H}_0$ allows the determination of a suitable detection threshold T in a Neyman-Pearson sense as

$$T = \text{erfc}^{-1}(2P_f) \sqrt{2\sigma_0^2} + \mu_0$$
(11)

where P_f denotes the desired probability of false alarm. Regarding the detection statistic parameters (μ_1, σ_1^2) under the alternative hypothesis $\mathcal{H}_1$, it can easily be shown that $\mu_1 = -\mu_0$ and $\sigma_1^2 = \sigma_0^2$ by remembering that now $\forall i : \mathbf{y}_i = \mathbf{x}_i + \alpha \mathbf{w}_i$.

Fig. 4. Kodak test images (RGB, 768×512 pixels)

Image	μ_0	$\hat{\mu}_0$	σ_0	$\hat{\sigma}_0$
Barn	-238.71	-239.39	805.58	800.72
Facade	-216.56	-216.51	658.74	637.65
Girl	-133.77	-133.30	372.45	350.54
House	-134.91	-134.23	254.95	244.17
Island	-353.10	-353.55	1609.80	1571.80
Parrots	-287.28	-285.25	1738.73	1657.28
Rafting	-185.94	-186.64	801.52	826.01
Window	-139.83	-140.59	986.03	984.52
Zentime	-349.46	-352.74	1491.52	1461.93

Table 1. Theoretical and experimental values of the detector statistics under $\mathcal{H}_0$.

4. EXPERIMENTAL RESULTS

For all reported results we take nine images of the widely used set of Kodak color images (see Fig. 4). We resize the images to 192×128 pixels (for a challenging detection scenario) and decompose the individual color bands of each image using the DWT with biorthogonal 7/9 wavelet filters and – without loss of generality – select the HL subbands at decomposition level two[1]. Before we start a comparative study of the detection performance, we have to verify two important assumptions in order to ensure a reasonable threshold selection. First, we verify that the detector responses under both hypothesis follow a Gaussian law by employing a Lilliefors test [12] at the 5% significance level. The normality assumption can not be rejected for all images. Second, we check if the theoretical values μ_0 and σ_0^2 are close to the experimental values we obtain from Eq. (9) and Eq. (10) under $\mathcal{H}_0$. Table 1 lists the corresponding theoretical (μ_0, σ_0^2) and experimental values $(\hat{\mu}_0, \hat{\sigma}_0^2)$. As we can see, the theoretical values are close to the estimated ones which ensures that the desired P_f is met. Since both assumptions hold, Eq. (11) can be used to calculate a detection threshold T. We decide to set the embedding strength $\alpha = 5$ for all subbands which ensures a PSNR of ≈ 46 dB for the luminance channel. For the computation of the PSNR of color images we average the Mean-Square Error (MSE) across all channels first. We compare the detection performance in terms of the probability of missing the watermark (P_m) for a fixed probability of false alarm ($P_f = 10^{-6}$). The mean and variance of the detection statistic are estimated experimentally under $\mathcal{H}_1$ from 1000 test runs for each image and $\hat{P}_m = \frac{1}{2} \text{erfc} \left((\hat{\mu}_1 - T) / \sqrt{2\hat{\sigma}_1^2} \right)$ is used to determine the empirical probability of missing the water-

---

[1]The MATLAB code for our watermarking scheme is available upon request at http://www.wavelab.at/sources.

Image	LC-L	LC-J	LC-KLT	LRT-GGD-L	MPE
Barn	10^{-6}	10^{-7}	10^{-27}	10^{-31}	$\mathbf{10^{-50}}$
Facade	0.46	0.35	10^{-5}	10^{-5}	$\mathbf{10^{-24}}$
Girl	0.97	0.97	0.43	10^{-95}	$\mathbf{10^{-103}}$
House	0.03	0.02	10^{-12}	10^{-8}	$\mathbf{10^{-22}}$
Island	10^{-9}	10^{-10}	10^{-42}	$\mathbf{10^{-189}}$	10^{-166}
Parrots	10^{-6}	10^{-6}	10^{-20}	10^{-70}	$\mathbf{10^{-86}}$
Rafting	0.21	0.15	10^{-7}	10^{-12}	$\mathbf{10^{-16}}$
Window	0.02	0.03	10^{-9}	10^{-54}	$\mathbf{10^{-79}}$
Zentime	0.12	0.06	10^{-10}	10^{-121}	$\mathbf{10^{-168}}$

Table 2. Empirical probability of missing the watermark ($\hat{P}_m$) at 46 dB PSNR for different detectors ($P_f = 10^{-6}$, 1000 test runs).

mark. Table 2 provides the results for the five detectors: the LC detector on the luminance (LC-L) channel, the LC detector operating on the joint RGB (LC-J) subbands, the LC detector operating on the KLT-decorrelated color-channels (LC-KLT), further the LRT conditioned on Generalized Gaussian modeled luminance coefficients (LRT-GGD-L) and the proposed MPE detector. The best results are marked bold. The LC-L and LC-J detector are described in [4], the LC-KLT detector is proposed in [1] and the LRT-GGD-L detector is analyzed in [3]. We adapted the respective watermarking schemes to work in the DWT domain. As we can see, the MPE detector performs better than the LRT-GGD-L detector, except for one image. It significantly outperforms the LC detectors, though. Further, we note that taking into account all color components improves detection performance (compare the improved performance of the LC-J and LC-KLT over the LC-L detector). The proposed MPE detector also compares favorable after common signal processing attacks. However, with increasing JPEG compression ratios the advantage of the MPE detector diminishes as the chromatic bands are heavily subsampled and quantized. We have to omit detailed results due to lack of space.

5. CONCLUSION

We proposed a novel detector for additive, spread-spectrum watermarking of color image DWT subbands based on the multivariate power-exponential distribution. This signal model allows to capture the highly correlated structure of the subbands. The derived likelihood ratio test achieves increased detection performance compared to watermarking the luminance channel only and earlier detectors based on a Gaussian host signal model.

A. APPENDIX

Proof of Eq. (10). Let X denote a random variable and k denote a constant. We want to determine the variance of $L(\mathbf{Y})$ (see Eq. 8) under $\mathcal{H}_0$ (i.e. $\mathbf{y}_i = \mathbf{x}_i$). Since the second summation term is a constant w.r.t. $\mathbf{w}_i$ and $\mathbb{V}(X + k) = \mathbb{V}(X)$ it follows that

$$\mathbb{V}(L(\mathbf{Y})) = \mathbb{V}\left(-\frac{1}{2}\sum_{i=1}^{m}\left((\mathbf{x}_i - \alpha\mathbf{w}_i)^T\mathbf{\Sigma}^{-1}(\mathbf{x}_i - \alpha\mathbf{w}_i)\right)^{\beta}\right). \quad (12)$$

By noting that the variance of a sum of i.i.d. random variables is the sum of the variances and since $\mathbb{V}(kX) = k^2\mathbb{V}(X)$, it follows that

$$\mathbb{V}(L(\mathbf{Y})) = \frac{1}{4}\sum_{i=1}^{m}\mathbb{V}\left(\left((\mathbf{x}_i - \alpha\mathbf{w}_i)^T\mathbf{\Sigma}^{-1}(\mathbf{x}_i - \alpha\mathbf{w}_i)\right)^{\beta}\right). \quad (13)$$

Next, we remember that $\mathbf{w}_i$ is our variable term following a discrete probability distribution with equiprobable values in $\{+1, -1\}$. The corresponding PDF is given by

$$\mathbb{P}(X = x) = f(x) = \begin{cases} 1/2 & \text{if } x = +1, \\ 1/2 & \text{if } x = -1, \end{cases} \quad (14)$$

then the variance $\mathbb{V}(X)$ follows as

$$\mathbb{V}(X) = \frac{1}{2}\left(\sum_{i=1}^{2}x_i^2 - \frac{1}{2}\left(\sum_{i=1}^{2}x_i\right)^2\right) \quad (15)$$

where $x_1 = -1$ and $x_2 = +1$. By substituting $x_1 = \left((\mathbf{x}_i - \alpha)^T\mathbf{\Sigma}^{-1}(\mathbf{x}_i - \alpha)\right)^{\beta}$ and $x_2 = \left((\mathbf{x}_i + \alpha)^T\mathbf{\Sigma}^{-1}(\mathbf{x}_i + \alpha)\right)^{\beta}$, we get

$$\mathbb{V}(L(\mathbf{Y})) = \frac{1}{16}\sum_{i=1}^{m}\left(\left[(\mathbf{x}_i + \alpha)^T\mathbf{\Sigma}^{-1}(\mathbf{x}_i + \alpha)\right]^{\beta} - \right.$$
$$\left. \left[(\mathbf{x}_i - \alpha)^T\mathbf{\Sigma}^{-1}(\mathbf{x}_i - \alpha)\right]^{\beta}\right)^2 \quad (16)$$

References $\square$

[1] M. Barni, F. Bartolini, A. De Rosa, and A. Piva, "Color image watermarking in the Karhunen-Loeve transform domain," *Journal of Electronic Imaging*, vol. 11, no. 1, pp. 87–95, Jan. 2002.

[2] Elisa Sayrol, Josep Vidal, Silvia Cabanillas, and Sonia Santamaría, "Optimum watermark detection in color images," in *Proceedings of the IEEE International Conference on Image Processing (ICIP'99)*, Kobe, Japan, Oct. 1999, vol. 2, pp. 231–235.

[3] Juan Ramon Hernández, Martín Amado, and Fernando Pérez-González, "DCT-domain watermarking techniques for still images: Detector performance analysis and a new structure," *IEEE Transactions on Image Processing*, vol. 9, no. 1, pp. 55–68, Jan. 2000.

[4] Mauro Barni, Franco Bartolini, and Alessandro Piva, "Multi-channel watermarking of color images," *IEEE Transactions on Circuits and Systems for Video Technology*, vol. 12, no. 3, pp. 142–156, Mar. 2002.

[5] Tsz Kin Tsui, Xiao-Ping Zhang, and Dimitrios Androutsos, "Color image watermarking using multidimensional fourier transforms," *IEEE Transactions on Information Forensics and Security*, vol. 3, no. 1, pp. 16–28, Mar. 2008.

[6] G. R. Nelson, G. A. Julien, and O. Yadid-Pecht, "CMOS image sensor with watermarking capabilities," in *Proceedings of the IEEE International Symposium on Circuits and Systems, ISCAS '05*, Kobe, Japan, May 2005, vol. 5, pp. 5326–5329, IEEE.

[7] Yufeng Liang, Eero Simoncelli, and Zhibin Lei, "Color channels decorrelation by ICA transformation in the wavelet domain for color texture analysis," in *Proceedings of the IEEE Conference on Computer Vision and Pattern Recognition, CVRP '00*. June 2000, vol. 1, pp. 606–611, IEEE.

[8] G. Verdoolaege and P. Scheunders S. De Backer, "Multiscale colour texture retrieval using the geodesic distance between multivariate Generalized Gaussian models," in *Proceedings of the IEEE International Conference on Image Processing (ICIP'08)*, San Diego, California, USA, 2008, pp. 169 – 172.

[9] S. Nadarajah, "The Kotz–type distribution with applications," *Statistics*, vol. 37, no. 4, pp. 341–358, July 2003.

[10] K. Zografos, "On Mardia's and Song's measures of Kurtosis in elliptical distributions," *Journal of Multivariate Analysis*, vol. 99, no. 5, pp. 858–879, May 2008.

[11] K.V. Mardia, "Measures of multivariate Kurtosis and Skewness," *Biometrika*, vol. 57, pp. 519–530, 1970.

[12] H. Lilliefors, "On the Kolmogorov-Smirnov test for normality with mean and variance unknown," *Journal of the American Statistical Association*, vol. 62, pp. 399–402, June 1967.